JOC Article

Examination of the Structural Features That Favor the Columnar Self-Assembly of Bis-urea Macrocycles

Jun Yang, Mahender B. Dewal, David Sobransingh, Mark D. Smith, Yuewen Xu, and Linda S. Shimizu*

Department of Chemistry and Biochemistry, University of South Carolina, Columbia, South Carolina 29208

shimizul@mail.chem.sc.edu

Received August 01, 2008

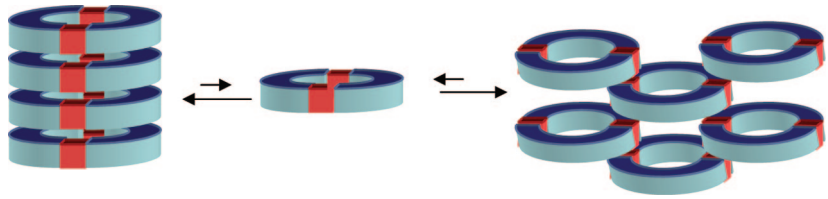

Second-generation self-assembling bis-urea macrocycles were designed that form columnar structures in the solid state. The new macrocycles were constructed from more flexible building blocks yielding greater solubility and a more efficient synthesis. In addition, heteroatoms in the form of ether oxygens were incorporated in the walls of the macrocycles to provide additional recognition sites for guest encapsulation. We observed reduced fidelity of the stacking motif and in some cases the intermolecular urea−urea hydrogen bonds were disrupted by the formation of intramolecular hydrogen bonds. We also observed new offset assembly motifs that maintained the urea−urea interaction. These results suggest that the stacking of the arene units in the rigid first-generation systems was an important factor in guiding the formation of the columnar stacks.

Introduction

It is fundamentally important for many applications in chemistry, biochemistry, and material science to understand how noncovalent forces guide the formation and stability of assembled and folded structures.[1] Of particular interest are directional forces, such as hydrogen bonding and metal−ligand interactions, that can predictably assemble molecules into discrete structures including cages, capsules, and rods.[2] The urea−urea hydrogen bonding interaction has proven to be a reliable and predictable self-assembling motif. Pioneering work by Etter et al. examined the assembly patterns of ureas by X-ray crystallography and formulated a set of empirical guidelines for predicting their assembly patterns.[3] This versatile 3-centered urea−urea motif has been employed to direct the formation of sheets,[4,5a] fibers,[5] polymers,[6] gels,[7] capsules,[8] and two-dimensional molecular solids.[9]

We have utilized the urea−urea interaction to design macrocycles that self-assemble into columnar structures with guest-

(1) (a) Goodman, C. M.; Choi, S.; Shandler, S.; DeGrado, W. F. *Nat. Chem. Biol.* **2007**, *3*, 252–262. (b) Ray, C. R.; Moore, J. S. *Adv. Polym. Sci.* **2005**, *177*, 91–149. (c) Fulop, F.; Martinek, T. A.; Toth, G. K. *Chem. Soc. Rev.* **2006**, *35*, 323–334. (d) Sakai, N.; Mareda, J.; Matile, S *Acc. Chem. Res.* **2005**, *38*, 79–87. (e) Berl, V.; Huc, I.; Khoury, R. G.; Lehn, J. M *Chem. Eur. J.* **2001**, *7*, 2798–2809.

(2) (a) Vriezema, D. M.; Aragones, M. C.; Elemans, J. A. A. W.; Cornelissen, J. J. L. M.; Rowan, A. E.; Nolte, R. J. M *Chem. Rev.* **2005**, *105*, 14451489. (b) Dybtsev, D. N.; Nuzhdin, A. L.; Chun, H.; Bryliakov, K. P.; Talsi, E. P.; Fedin, V. P.; Kim, K *Angew. Chem., Int. Ed.* **2006**, *45*, 916–920.

(3) Etter, M. C.; Urbanczyk-Lipkowska, Z.; Zia-Ebrahimi, M.; Panunto, T. W. *J. Am. Chem. Soc.* **1990**, *112*, 8415–8426.

(4) (a) Custelcean, R. *Chem. Commun.* **2008**, 295–307. (b) Davis, R.; Berger, R.; Zentel, R. *Adv. Mater.* **2007**, *19*, 3878–3881.

(5) (a) Palacin, S.; Chin, D. N.; Simanek, E. E.; MacDonald, J. C.; Whitesides, G. M.; McBride, M. T.; Palmore, G. T. R. *J. Am. Chem. Soc.* **1997**, *119*, 11807–11816. (b) Lovinger, A. J.; Nuckolls, C.; Katz, T. J. *J. Am. Chem. Soc.* **1998**, *120*, 264–268. (c) Castellano, R. K.; Nuckolls, C.; Eichhorn, S. H.; Wood, M. R.; Lovinger, A. J.; Rebek, J. *Angew. Chem., Int. Ed.* **1999**, *38*, 2603–2606.

(6) (a) Sijbesma, R. P.; Beijer, F. H.; Brunsveld, L.; Folmer, B. J. B.; Hirschberg, J. H. K. K.; Lange, R. F. M.; Lowe, J. K. L.; Meijer, E. W. *Science* **1997**, *278*, 1601–1604. (b) Castellano, R. K.; Clark, R.; Craig, S. L.; Nuckolls, C.; Rebek, J. *Proc. Natl. Acad. Sci. U.S.A.* **2000**, *97*, 12418–12421.

(7) (a) van Esch, J.; De Feyter, S.; Kellog, R. M.; De Schryver, F.; Feringa, B. L. *Chem. Eur. J.* **1997**, *3*, 1238–1243. (b) van Esch, J.; Kellogg, R. M.; Feringa, B. L. *Tetrahedron Lett.* **1997**, *38*, 281–284. (c) Carr, A. J.; Melendez, R.; Geib, S. J.; Hamilton, A. D. *Tetrahedron Lett.* **1998**, *39*, 7447–7450. (d) Jeong, Y.; Hanabusa, K.; Masunaga, H.; Akiba, I.; Miyoshi, K.; Sakurai, S.; Sakurai, K. *Langmuir* **2005**, *21*, 586–594. (e) Suzuki, M.; Nakajima, Y.; Yumoto, M.; Kimura, M.; Shirai, H.; Hanabusa, K. *Langmuir* **2003**, *19*, 8622–8624. (f) Estroff, L. A.; Hamilton, A. D. *Angew. Chem., Int. Ed.* **2000**, *39*, 3447–3450. (g) Wang, G.; Hamilton, A. D. *Chem. Eur. J.* **2002**, *8*, 1954–1961. (h) Jung, J. H.; Ono, Y.; Shinkai, S. *Chem. Eur. J.* **2000**, *6*, 4552–4557. (i) Moreau, J. J. E.; Vellutini, L.; Wong Chi Man, M.; Bied, C. *J. Am. Chem. Soc.* **2001**, *123*, 1509–1510.

10.1021/jo801717w CCC: $40.75
Published on Web 12/05/2008

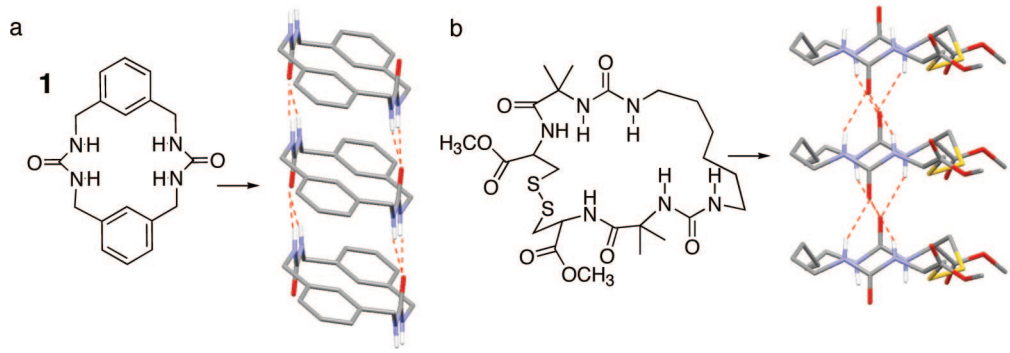

FIGURE 1. Examples of rigid and flexible macrocyclic bis-ureas that stack into columnar structures: (a) the *m*-xylene bis-urea **1**[12] and (b) L-cystine-based bis-ureas from Ranganathan et al.[14]

accessible channels.[10,11] The first generation of macrocycles contained two urea groups separated by two rigid aromatic units (spacers). These systems all assembled with high fidelity into the desired columnar structures even when the sizes and angles of the rigid spacer units were varied from *m*-xylene, 4,4′-dimethyl-diphenylether, to 4,4′-dimethylbenzophenone.[10−12] For example, Figure 1a shows the solid-state structure of the *m*-xylene macrocycle. The individual macrocycles are held together by three-centered urea hydrogen bonds that display H···O distances from 1.98 to 2.21 Å. The two ureas are oriented oppositely to minimize dipole interactions and are tilted slightly (26° from perpendicular) to bring the phenyl groups closer within the optimal distance 3.3 Å for the slip-stacked aryl interactions.[13]

In contrast to our rigid bis-urea macrocycles, Ranganathan and others reported that more flexible bis-ureas could also form columnar assemblies in the solid state (Figure 1b).[14−17] For example, the tubular assembly of the L-cystine-based bis-urea macrocycles from Ranganathan and Karle persuaded us to investigate more flexible, functionalized spacers in our own bis-urea systems. These macrocycles assembled into columnar structures from $CHCl_3$/MeOH in which the different spacer units self-segregated with the disulfide-containing spacer aligned on one side of the column and the alkyl group stacked on the opposite side (space group $P1$ with $Z = 1$, Figure 1b).[14] These examples are intriguing because they suggest that the urea−urea hydrogen bonding interaction is sufficiently robust and can direct the assembly of asymmetric and flexible macrocycles in the presence of heteroatoms.

In this paper, we study the assembly of a second generation of bis-urea macrocycles that are unsymmetrical and more flexible and contain additional heteroatoms. We are interested in the incorporation of these features because the heteroatoms provide additional recognition sites, which can line the columnar channel. The incorporation of flexible units and asymmetry into the macrocycles should improve their solubility and also increase the yields of the cyclization step. In the first generation rigid macrocycles, the yields of the macrocyclization were very low, typically 5−20%. Their poor solubility also limited the conditions that could be used to assemble the macrocycles to the most aggressive solvents such as DMSO, DMF, or AcOH. Better macrocycle solubility would increase the number of solvents that could be used for assembly. The enhanced solubility also enabled the study of the assembly of the macrocycles in solution.

These studies also yield some insight into how noncovalent forces influenced the assembly of the macrocycles into oligomers and further to solid-state structures. Our previously reported symmetrical bis-urea macrocycles have thus far been observed to form only columnar structures; however, an alternative urea−urea assembly could also yield offset structures (Figure 2). We made conservative changes, by replacing only one of the two rigid aromatic spacers from the first generation macrocycles with flexible aliphatic spacers to form unsymmetrical bis-urea macrocycles (Scheme 1). The introduction of asymmetry into the macrocyclic framework leads to additional types of assembled columns. One column aligns the spacers and a second possible column that alternates the position of the two spacer elements, similar to what was observed in the L-cystine-based bis-ureas.[14] We investigated how systematic alterations in the macrocycle framework affect the type and frequency with which different patterns are observed. Finally, we focused on whether one can discern any general guidelines from these simple models for the design of the next generation materials.

Results and Discussion

Our symmetrical macrocycles were formed from two identical rigid aromatic spacers and two urea groups.[12,18] In the new macrocycles, we systematically replace one of the aromatic spacers to improve solubility, increase the macrocyclization yields, and incorporate additional recognition sites that can interact with guests in the cavity. As a consequence the new macrocycles are unsymmetrical with one aromatic spacer unit

(8) Shimizu, K. D.; Rebek, J. *Proc. Nat. Acad. Sci. U.S.A.* **1995**, *92*, 12403–12407.
(9) (a) Shao, X.; Chang, Y.-L.; Fowler, F. W.; Lauher, J. W. *J. Am. Chem. Soc.* **1990**, *112*, 6627–6634. (b) Schauer, C. L.; Matwey, E.; Fowler, F. W. *J. Am. Chem. Soc.* **1997**, *119*, 10245–10246. (c) Hollingsworth, M. D.; Brown, M. E.; Satarsiero, B. D.; Huffman, J. C.; Goss, C. R. *Chem. Mater.* **1994**, *6*, 1227–1244.
(10) (a) Yang, J.; Dewal, M. B.; Shimizu, L. S. *J. Am. Chem. Soc.* **2006**, *128*, 8122–8123. (b) Yang, J.; Dewal, M. B.; Profeta, S.; Smith, M. D.; Li, Y. Y.; Shimizu, L. S. *J. Am. Chem. Soc.* **2008**, *130*, 612–621.
(11) Dewal, M. B.; Xu, Y.; Yang, J.; Mohammed, F.; Smith, M. D.; Shimizu, L. S. *Chem. Commun.* **2008**, 3909–3911.
(12) Shimizu, L. S.; Smith, M. D.; Hughes, A. D.; Shimizu, K. D. *Chem. Commun.* **2001**, 1592–1593.
(13) Meyer, E. A.; Castellano, R. K.; F, D. *Angew. Chem., Int. Ed.* **2003**, *42*, 1210–1250.
(14) Ranganathan, D.; Lakshmi, C.; Karle, I. L. *J. Am. Chem. Soc.* **1999**, *121*, 6103–6107.
(15) Semetey, V.; Didierjean, C.; Briand, J. P.; Aubry, A.; Guichard, G. *Angew. Chem., Int. Ed.* **2002**, *41*, 1895–1898.
(16) Hemmerlin, C; Marraud, M.; Rognan, D.; Graff, R.; Semetey, V.; Briand, J.-P.; Guichard, G. *Helv. Chim. Acta* **2002**, *85*, 3692–3711.
(17) (a) Harris, K. D. M. *Chem. Soc. Rev.* **1997**, *26*, 279–289. (b) Harris, K. D. M. *Supramol. Chem.* **2007**, *19*, 47–53.
(18) Shimizu, L. S.; Hughes, A. D.; Smith, M. D.; Davis, M. J.; Zhang, B. P.; zur Loye, H.-C.; Shimizu, K. D. *J. Am. Chem. Soc.* **2003**, *125*, 14972–14973.

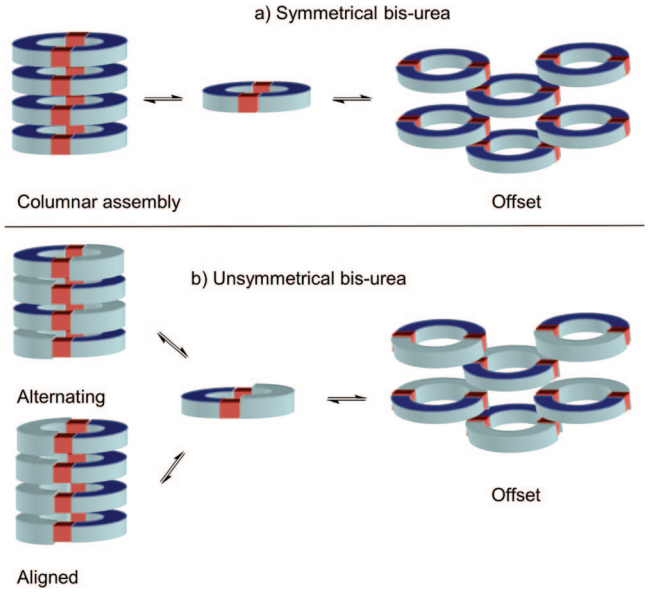

FIGURE 2. Schematic representation of the likely assembly patterns of bis-urea macrocycles formed from the assembly of the urea groups (shown in red) into columnar or offset structures: (a) symmetrical macrocycles and (b) unsymmetrical macrocycles.

and one aliphatic spacer unit. Scheme 1 shows the five new bis-ureas macrocycles **2**−**6**. Macrocycle **2** contained one aromatic *m*-xylene spacer and a conformationally flexible ethylene glycol spacer with two ether oxygens. The macrocycle **3** contained a longer ethylene glycol spacer to study the effects of increased macrocycle size and increased flexibility. Macrocycle **4** contained a simple octyl bridge with the same number of atoms as in macrocycle **2** but without the ether oxygens in order to study the influence of the heteroatoms on the assembly patterns. Structure **5** explored the effects of enhanced rigidity of the aromatic spacer. The *m*-xylene spacer of **3** was replaced with a 1,3-diaminobenzene spacer. Macrocycle **6** introduces an *o*-methyl as an additional steric constraint upon the 1,3-diaminobenzene spacer, which should impact the conformation of the adjacent urea group.

Slow simultaneous addition of the commercial diisocyanates and diamines gave good yields of most of these macrocycles (53−78%). In addition the macrocycles could be synthesized in a single step without need for urea protecting groups. In contrast in our first generation rigid macrocycles, a triazinanone protecting group was required to aid in the isolation and purification due to their poor solubility.[12] This added two additional steps, protection and deprotection, to the synthesis. All of the new unsymmetrical bis-ureas were much more soluble and could be readily purified by column chromatography (10:1 CH_2Cl_2/MeOH). Only macrocycle **5** showed low yield (14%).

We attribute the higher yields and solubility of these unsymmetrical macrocycles to the greater flexibility of the diamines, which likely aids in the macrocyclization step. The greater solubility also experimentally suggests that the urea self-association interactions in these more flexible systems may be considerably weaker than the rigid macrocycles. We next examined the solid-state structures of these different derivatives to determine any trends in their assembly patterns.

Solid-State Structures. Although the greater flexibility and presence of heteroatoms offer many advantages, including increased solubility and higher synthetic yields, they can also potentially disrupt the self-assembly process. Heteroatoms

SCHEME 1. Synthesis of Unsymmetrical Bis-urea Macrocycles 2−6

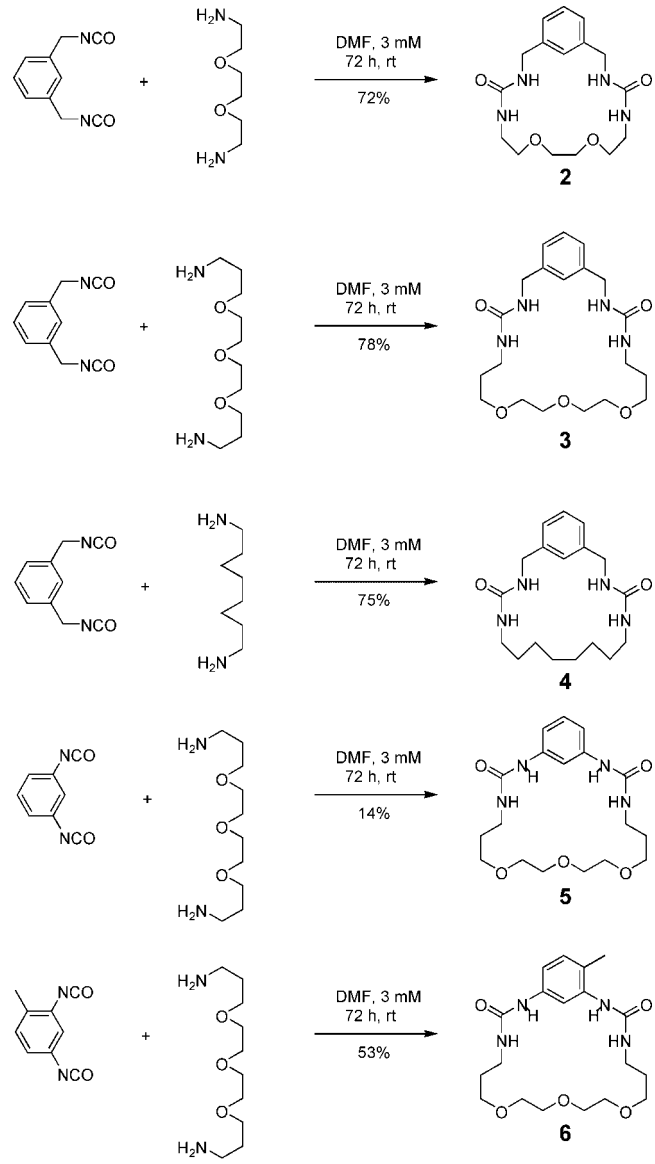

introduce additional inter- and intramolecular assembly motifs and the increased flexibility enables greater access to a larger number of conformations. To examine the assembly process more carefully, we attempted to grow single crystals of these new macrocycles from a number of solvents by slow evaporation. This approach allowed us to determine the fidelity of the assembly process.

Replacement of one of the two *m*-xylene rigid spacers in **1** with a 2,2′-(ethylenedioxy)diethyl unit afforded macrocycle **2**, which introduces both flexibility and heteroatoms in the form of a glycol bridge. Macrocycle **2** formed crystals from AcOH and from a 10:1 mixture of CH_2Cl_2/MeOH. While two different polymorphs were observed, each of these assembled structures maintained the urea−urea interaction. First, we will examine the structure obtained by slow evaporation from glacial acetic acid (30 mg/0.5 mL) solution (Figure 3a). The molecular unit contained no solvent and revealed the expected 19-membered bis-urea macrocycle. The macrocycles stack into columns similar to the more rigid macrocycle **1**. The two urea groups were also oriented in opposite directions as was observed in **1**, which

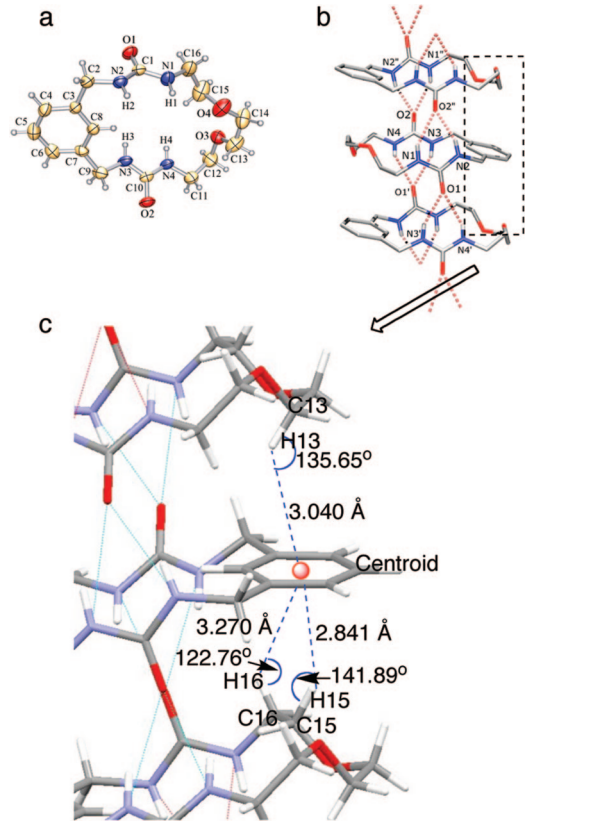

FIGURE 3. X-ray crystal structure of **2** from AcOH. (a) The molecular structure (**2a**) with displacement ellipsoids drawn at the 40% probability level. (b) Packing structure shown along the crystallographic [100] (*a* axis) direction. (c) Analysis of C−H···center of π-ring distances (<3.0 Å).

minimizes the net dipole, and the ureas were tilted ~34° from the perpendicular. The presence of the oxygen atoms did not appear to disrupt the assembly. The urea−urea hydrogen bonds formed in preference to any intra- or intermolecular NH to ether oxygen interactions. The urea NH to urea carbonyl oxygens (O(1) and O(2)) distances were shorter (2.09−2.27 Å) than the distance from the urea NH to ether oxygens (O(3) and O(4)) distances (2.62−2.86 Å).

Given the different lengths and thickness of the aliphatic and aromatic spacer units, it was not surprising that macrocycle **2** assembled into an alternating structure with the aromatic spacer of one macrocycle sandwiched between the ethylene glycol spacers of the neighboring macrocycles. This alternating assembly forms CH···π interactions in lieu of the aromatic interactions observed with **1**. The CH···π interactions (Figure 3c) have distances that range from 2.8 to 3.3 Å (from H to centroid of aryl ring) and CH···π angles range from 123°−142° (from C−H to centroid of aryl ring). Like the π−π stacking interactions in **1**, the CH···π interactions might assist in stabilizing the columnar arrangement of **2a**. Alternatively, the choice of CH···π interactions over π−π interactions may simply be due to packing considerations and perhaps one gives an optimal space filling.

With the symmetrical, rigid bis-urea macrocycles such as **1**, we had previously only observed a single columnar assembly with each macrocycle. We were therefore surprised to observe a polymorph of **2**, which formed from a 10:1 mixture of CH_2Cl_2/MeOH. These colorless cubic shape crystals of macrocycle **2** adopted conformation **2b** (Figure 4a), and no solvent was

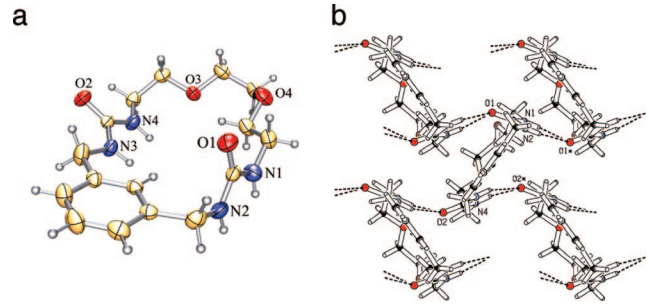

FIGURE 4. X-ray crystal structure of **2** from CH_2Cl_2/MeOH solution. (a) Molecular structure (**2b**) with displacement ellipsoids drawn at the 40% probability level. (b) Packing structure in which each molecule is linked to four equivalent molecules via NH···O hydrogen bonds through the urea groups. The offset packing pattern created two-dimensional herringbone packed layers in the crystallographic (ac) plane.

included in the crystals. Again, the assembly is organized by the typical three-centered urea motif, with similar NH···O distances ranging from 2.05 to 2.25 Å. The urea self-association appears to be stronger than the NH-ether oxygen interactions. Although one of the ether oxygens O(3) formed a hydrogen bond with one of the ureas with a NH(4)···O(3) distance of 2.34 Å.

The primary difference in polymorph **2b** is that instead of forming columns, the macrocycle assembled into an offset pattern. Figure 4b illustrates the 2D herringbone packed layers where one macrocycle was hydrogen bonded to four other macrocycles. The rigid aromatic spacers point to one direction and the flexible polyethylene glycol spacers point to the opposite direction. Surprisingly, there appears to be no effective π−π stacking or CH···π interaction in this association. This offset polymorph maybe due to the different molecular conformation of the macrocycle in which the urea groups are both pointing in the same direction.

The ethylene glycol spacer indeed gave macrocycle **2** increased conformational freedom and higher solubility versus the rigid macrocycle **1**. To compare the two conformations of **2**, we imported the X-ray structure data into Spartan.[19] Each structure was frozen, and the molecular energies were calculated using Hartree−Fock models with 3-21G basis set. Conformation **2b** was predicted to be lower in energy but the difference between the total energy was small (4.77 kJ/mol). It is likely that macrocycle **2** samples a number of conformations, rapidly interconverting between **2b** and **2a** in solution.

To investigate the effects of the two oxygens in the ethylene glycol linker on the hydrogen bonding patterns, we calculated the surface potentials for both conformations. Figure 5 shows that the carbonyl oxygens in both conformations have the larger calculated surface potentials (−66.6 to −69.9 kJ/mol) versus the ether oxygens (−32.8 to −46.5 kJ/mol) and appear to be the best hydrogen bond acceptors. Such rankings of hydrogen bond donors and acceptors based on their molecular electrostatic potentials have been used by Aakeroy et al. to predict hydrogen-bonding pairs.[20] Yet, particularly in polymorph **2a**, one of the NH groups was visibly twisted toward one of the ether oxygens, indicating the presence of a weak interaction.

(19) *Spartan 04 for Macintosh*, v 1.1.1; Wavefunction, Inc.: Irvine, CA., 2007.

(20) Aakeroy, C. B.; Schultheiss, N.; Desper, J.; Moore, C. *Cryst. Growth Des.* **2007**, *7*, 2324–2331.

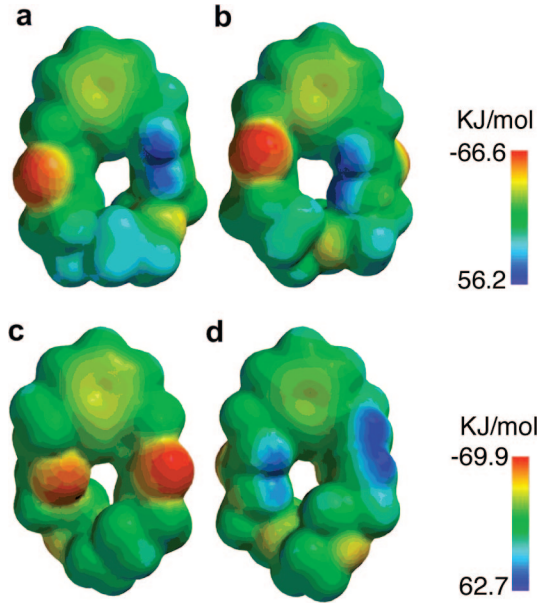

FIGURE 5. Calculated surface potentials of macrocycle **2**. (a) Front view of structure **2a** of the crystal obtained from AcOH. (b) Back view of structure **2a**. (c) Front view of structure **2b** of the crystal obtained from CH_2Cl_2/MeOH. (d) Back view of structure **2b**.

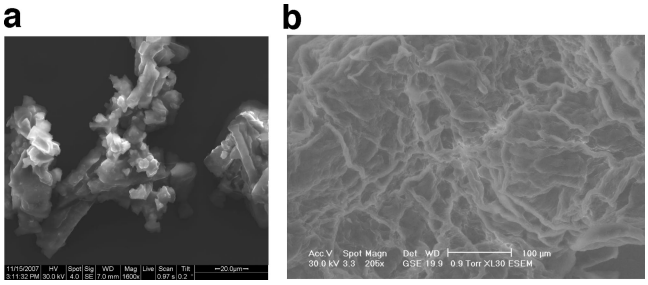

FIGURE 6. SEM images of dried xerogels of macrocycle **3** in $CHCl_3$ (a) near the MGC of 1.2 M and (b) at a higher concentrations (2.5 M).

We next examined the effect of increasing the length of the ethylene glycol spacer. The larger macrocycle **3** had a significantly lower melting point (163−165 °C) compared with that of macrocycle **2** (mp 247−250 °C) and improved solubility in organic solvents, properties that were consistent with a decrease in the strength of the noncovalent intermolecular interactions. Surprisingly, we were unable to grow crystals of **3** from any solvent system. Instead macrocycle **3** formed gels in a wide range of organic solvents including $CHCl_3$, CH_2Cl_2, $CHCl_2CHCl_2$, benzene, toluene, MeOH, EtOH, and AcOH. The SEM images of the gels with $CHCl_3$ (Figure 6) indicated that elongated linear aggregates were formed and the linear aggregates were entangled to create junction zones. These structures suggest that macrocycle **3** may form linear aggregates. The minimum gel concentration (MGC) was measured by the "tube inversion" method (Table 1) and was found to be ∼100-fold higher than the acyclic bis-urea gelators.[21,7] These acyclic bis-ureas gelators are typically composed of aryl ureas and long hydrophobic chains. Interestingly, **3** does not appear to fit this model as it is cyclic and contains an ethylene glycol spacer.

TABLE 1. Minimum Gel Concentrations (MGC) of Macrocycle 3 in Organic Solvents

solvent	MGC (g/L)
$CHCl_3$	512
CH_2Cl_2	105
$CHCl_2CHCl_2$ (TCE)	1584
MeOH	1072
EtOH	419
AcOH	2200
benzene	56
toluene	<70

Comparison of macrocycles **2** versus **3** and their assembly propensities demonstrated that the smaller, less flexible ring of **2** is better suited to form columnar structures in the solid state. To examine whether the larger macrocycle may be prone to collapse or to adopt other possible intra- and intermolecular interactions, we turned to molecular models. A Monte Carlo search on the monomer **3** using Spartan[19] with MMFF predicted that the lowest energy structures have intramolecular hydrogen bonding from three of the urea NHs to ether oxygens (Figure 7a), although the calculated surface potential of macrocycle **3** (Figure 7b,c) still identifies the urea carbonyl oxygens as the best hydrogen bond acceptor. The predicted intramolecular distances for the NH to ether oxygens range from 1.93 to 2.11 Å. These intramolecular hydrogen bonds pull the flexible chain close to the rigid spacer to form entropically favorable six-membered ring structures and limit the cavity size. Such strong intramolecular hydrogen bonds would nicely account for the lower melting point and greater solubility of **3**, as it would make the intermolecular urea interactions weaker. Macrocycle **3** associates into complex structures forming gels. These results suggest that it may not be possible to make larger flexible systems assemble into columnar structures.

To examine what effect the additional ether oxygen heteroatoms have on the assembly pattern, we investigated macrocycle

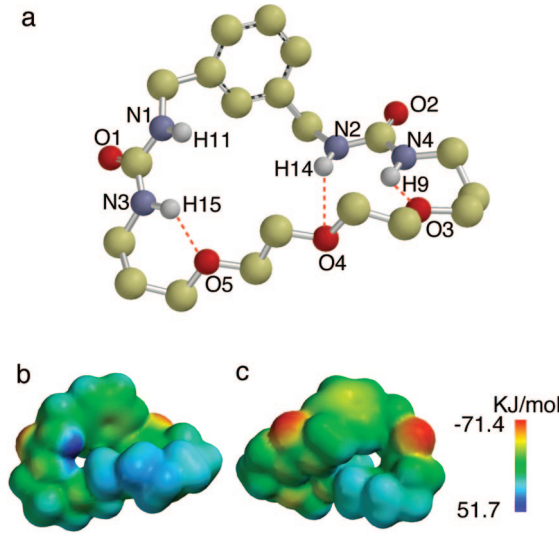

FIGURE 7. Calculated molecular structures of macrocycle **3**. (a) Lowest energy conformer identified from a Monte Carlo search (hydrogens omitted for clarity). (b) Calculated surface potential of macrocycle **3** (front view). (c) Calculated surface potential of macrocycle **3** (back view). Calculate surface potentials for oxygen acceptors: carbonyl O1, ∼ −70.4; carbonyl O2, ∼ −70.2; O3, ∼ −39.7; O4, ∼ −29.9; O5, ∼ −24.8.

(21) (a) Shi, C.; Huang, Z.; Kilic, S.; Xu, J.; Enick, R. M.; Beckman, E. J.; Carr, A. J.; Melendez, R. E.; Hamilton, A. D. *Science* **1999**, *286*, 1540–1543. (b) van, E., J; Schoonbeek, F.; de, L., M; Kooijman, H.; Spek, A. L.; Kellogg, R. M.; Feringa, B. L. *Chem. Eur. J.* **1999**, *5*, 937–950. (c) van, E., J; Schoonbeek, F.; de, L., M; Kooijman, H.; Spek, A. L.; Kellogg, R. M.; Feringa, B. L. *Chem. Eur. J.* **1999**, *5*, 937–950. (d) Yabuuchi, K.; Marfo-Owusu, E.; Kato, T. *Org. Biomol. Chem.* **2003**, *1*, 3464–3469. (e) Fages, F.; Vogtle, F.; Zinic, M. *Top. Curr. Chem.* **2005**, *256*, 77–131.

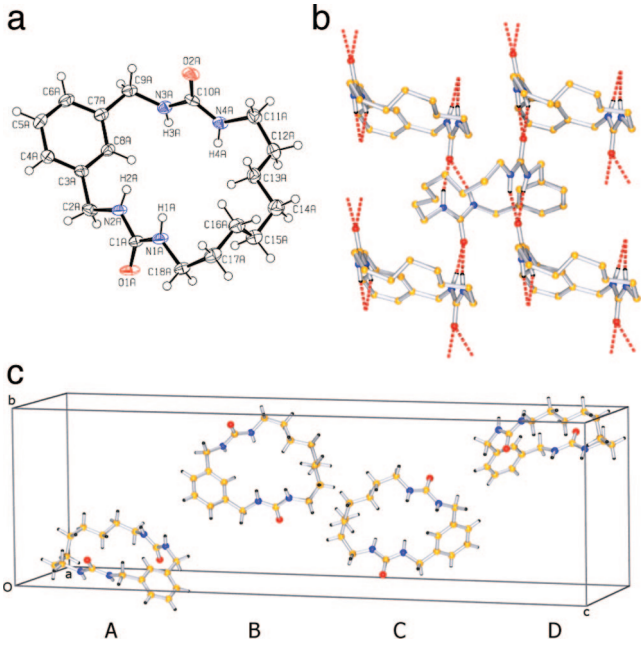

FIGURE 8. X-ray crystal structure of macrocycle **4**. (a) Ellipsoid plots of the four independent molecules with displacement ellipsoids drawn at the 50% probability level. (b) Local hydrogen bonding environment. Each molecule links four others in a 2D sheet structure. (c) The asymmetric unit of the crystal contains four crystallographically independent, chemically identical molecules. Atom labeling differs only in suffix A−D.

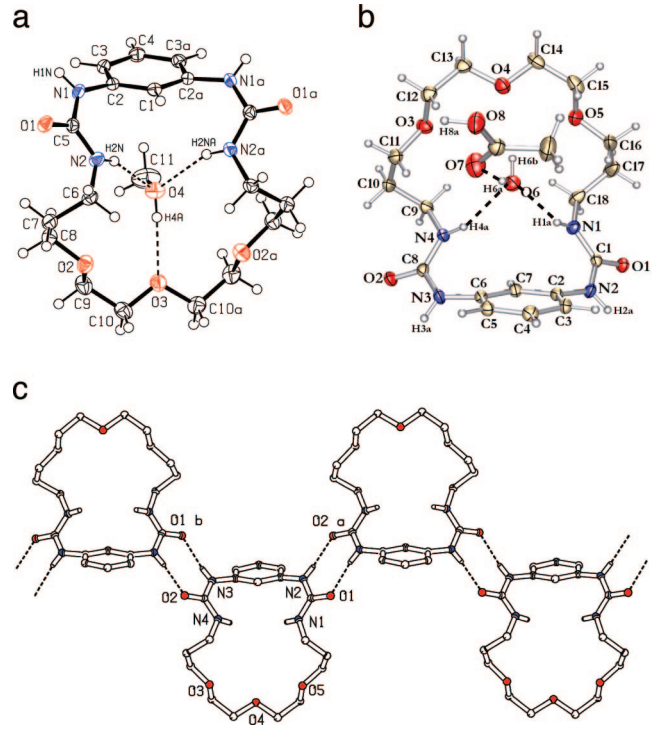

FIGURE 9. X-ray crystal structures of macrocycle **5** crystallized from (a) MeOH and from (b) AcOH. Hydrogen bonds involving the MeOH guest are shown. (Displacement ellipsoids drawn at the 50% probability level). (c) Packing structure of macrocycle **5** with AcOH and H_2O guests omitted. Cycles link into infinite 1D chains along the crystallographic *b* axis via NH···O hydrogen bonds.

4, which had the same length flexible spacer as **2** but without the heteroatoms. Bis-urea **4** crystallized into identical offset structures from a large variety of solvents (CH_2Cl_2/MeOH, AcOH, MeOH, DMSO/H_2O, or DMSO/hexanes). The corresponding polymorphs with aligned columnar structures were not observed. Figure 8b showed the assembled structure of **4** obtained from slow evaporation from mixture of CH_2Cl_2/MeOH. The two urea groups from a single macrocycle point in opposite directions (Figure 8a). Macrocycle **4** adopted an extended 2D sheet network through hydrogen bonds (Figure 8b). The asymmetric unit of the crystal contains four crystallographically independent but chemically identical molecules (A−D, Figure 8c). The association of A/C and B/D molecules of the asymmetric unit cell created sheets (Supporting Information). Each molecule of **4** was connected to four others through 3-centered urea hydrogen bonding. The hydrogen bond distances range from 1.98−2.18 Å. The aromatic spacers were oriented on the same side of the sheet; however, the measured centroid distances between the benzene groups was ∼4.6 Å, too far for any substantial $\pi-\pi$ interaction because the octyl groups were interdigitated, filling the empty internal space of the macrocyclic monomers. The predominantly offset assembly pattern in **4** appears to indicate that the added noncovalent interactions, including aryl stacking in **1** and CH···π interactions in **2** were actually quite important in aligning the macrocycles into the stacked columnar structures as opposed to the offset patterns.

We next examined whether the large flexible ethylene glycol spacer used in macrocycle **3** could be coaxed back into a crystalline columnar assembly by increasing the rigidity of the aromatic spacer. We replaced the *m*-xylene spacer of **3** with a more rigid 1,3-phenyl spacer while keeping the ethylene glycol spacer unchanged to give macrocycle **5**. This modification also increased the acidity of the ureas. In contrast to macrocycle **3**, macrocycle **5** crystallized from both AcOH and MeOH into very similar structures. Surprisingly, neither of these structures displayed the typical 3-centered urea interactions, and both showed inclusion of solvent molecules (Figure 9a,b) within the macrocycles. The urea groups adopt *cis*/*trans*-conformations, as unexpectedly observed in urea-containing pseudopeptides[22] and more commonly seen with thioureas.[23] One pair of urea NHs formed hydrogen bonds with the included solvent, and several ether oxygens also formed stabilizing interactions. The aryl NHs adopted a *cis*-conformation and pointed outside the macrocycle. These *cis* NHs are used to knit individual monomers together in a ribbon structure through amide−amide-type hydrogen bonds (Figure 9c). The inclusion complexes demonstrate that we can get additional recognition of guests inside the channel. Unfortunately, the inclusion complex disrupted the desired urea−urea interactions and the formation of the columnar assembly.

Introduction of an *o*-methyl group to the aryl spacer (2,4-toluenediisocyanate) in **5** gave macrocycle **6**. We predicted that this simple steric constraint would induce a more favorable perpendicular alignment of the urea group, thus encouraging columnar assembly. Indeed, Bouteiller found that soluble assemblies formed from bis-ureas synthesized from this 2,4-toluenediamine precursor with reduced solubility observed for the compound lacking the methyl group.[24] Colorless needle-

(22) Semetey, V.; Hemmerlin, C.; Didierjean, C.; Schaffner, A. P.; Giner, A. G.; Aubry, A.; Briand, J. P.; Marraud, M.; Guichard, G. *Org. Lett.* **2001**, *3*, 3843–3846.

(23) (a) Custelcean, R. *Chem. Commun.* **2008**, 295–307. (b) Custelcean, R.; Gorbunova, M. G.; Bonnessen, P. V. *Chem. Eur. J.* **2005**, *11*, 1459–1466.

(24) (a) Boileau, S.; Bouteiller, L.; Laupretre, F.; Lortie, F. *New J. Chem.* **2000**, *24*, 845–848. (b) Lortie, F.; Boileau, S.; Bouteiller, L.; Chassenieux, C.; Deme, B.; Ducouret, G.; Jalabert, M.; Laupretre, F.; Terech, P. *Langmuir* **2002**, *18*, 7218–7222.

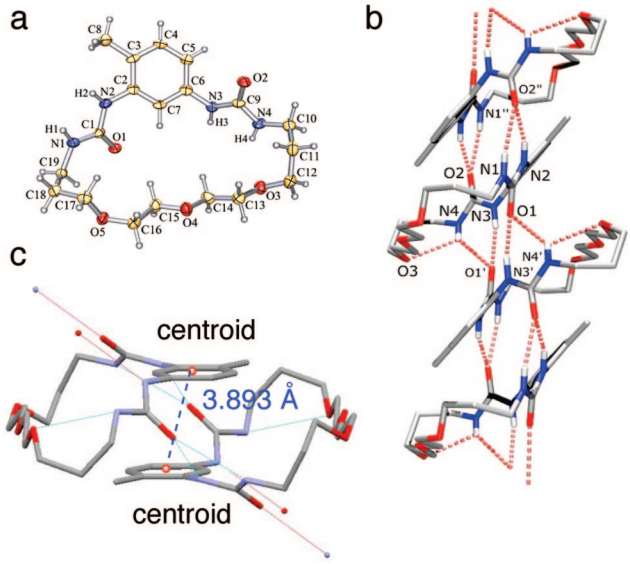

FIGURE 10. Depictions of (a) the molecular unit, (b) packing structure and (c) the $\pi-\pi$ stacking distance in the dimeric unit of the X-ray structure of macrocycle **6**.

shaped single crystals of **6** were obtained by slow evaporating of its CH_2Cl_2/MeOH (10:1) solution. The crystal structure confirmed assembly of macrocycle **6** into the columnar arrangement with strong urea−urea interactions (Figure 10a,b). Gratifyingly, both urea groups adopted an all-*trans* conformation and were oriented in opposite directions. A weak intramolecular hydrogen bond between N(4)−H(4)···O(3) was observed with bond length 2.44 Å. This internal hydrogen bond shrinks the cavity size of the cycle, and no solvent was included within the channel. On the opposite side of the ring the second urea NH(1) is too far (~4.23 Å) from the ether O(5) to form an effective interaction.

Indeed, it seems as if the simple steric constraint of the *o*-methyl group was enough to tip the balance back toward the columnar assembly pattern. The macrocycles were stacked in alternating directions along the crystallographic *a* axis (Figure 10c). The column was actually formed from two macrocycles that are dimerized together via urea−urea and the $\pi-\pi$ stacking interactions. Surprisingly, the π-stacking interactions formed between the two phenyl groups in the dimer that are on opposite sides of the column. The centroid distance between these two phenyl groups is 3.89 Å and the perpendicular distance between two phenyl rings is 3.49 Å (Figure 10c). These dimers are then stacked on top of each other held together by strong urea−urea interactions. Specifically, NH(3′) formed a strong hydrogen bond to carbonyl oxygen O(1) with an H(3′)···O(1) distance of 1.92 Å.

In our investigation of the crystal structures of a series of unsymmetrical bis-urea macrocycles **2**−**6**, we found that although the urea−urea interactions were predominant, they did not always lead to the desired columnar assemblies. The offset structures were actually more common than the columnar assemblies. The flexibility of these systems and the inclusion of the ether oxygens gave rise to many additional assembly patterns. Thus very subtle changes such as the inclusion of a single methyl group shifted the structure from one assembly pattern to another. Even though these flexible macrocycles have reduced, we were still able to observe the desired columnar structures. For example, macrocycles **2** and **6** formed columns of macrocycles that were stacked. We predict that other heteroatoms may also be accommodated within a rigid framework without disrupting the columnar assembly.

Solution Studies. In contrast to the previous generation of rigid, symmetrical macrocycles, the new flexible macrocycles showed greatly enhanced solubility. For the first time, we examined the assembly of our bis-urea macrocycles in solution and measured their association constants. We were particularly interested in how the presence of heteroatoms would affect the strength of the macrocycle-macrocycle association constant. We expected to see lower association constants for the macrocycles that could form intramolecular hydrogen bonds, because the intramolecular hydrogen bonds would compete with the intermolecular urea−urea interactions.

The unsymmetrical bis-ureas **2**−**4** were soluble in $CHCl_3$, CH_2Cl_2, and 1,1,2,2,-tetrachloroethane (TCE), exhibiting the highest solubilities in TCE. As expected, ^{1}H experiments with **2**−**4** in TCE-d_2 revealed a downfield shift of 0.2 to 0.6 ppm of the urea protons with increasing concentration (Figure 11). This was consistent with the formation of hydrogen bonding interactions between the urea NHs. All the bis-ureas show a plateau at the lower concentration range from 0.5−1.0 mM, suggesting that they are unassociated monomers at these concentrations. No plateau was observed at higher concentrations, indicating that the association did not reach equilibrium even in saturated solution, which is an indication of low association constants. Macrocycle **3** appeared to be monomeric over a slightly higher concentration range 1.0−2.5 mM. It also showed no plateau at higher concentrations.

The ^{1}H studies indicated that **2** and **3** have some intramolecular hydrogen bonding interactions in the unassociated (monomer) form based on the comparison of the chemical shifts of **2** and **3** versus **4** at low concentrations. The NHs of **2** and **3**, which can form intramolecular hydrogen bonds, are much further downfield than the NHs in **4**, which cannot form intramolecular hydrogen bonds because it lacks ether oxygens. However, ^{1}H did not yield a clear measure of the binding interactions.

Therefore, we turned to IR to examine the assembly process further. The free urea N−H bond stretching band and the hydrogen-bonded urea N−H band are well separated and suitable for quantitative analysis.[25] In fact, one can differentiate by IR between the typical 3-centered urea (*trans*/*trans*) hydrogen bonding interaction in which both urea NH's begin to form hydrogen bonds versus *cis*/*trans* conformation in which only one NH-participates in hydrogen bonding.[26]

FT-IR studies with macrocycle **2** showed the free urea N−H stretching at 3448 cm^{-1} and hydrogen-bonded N−H stretching band at 3358 cm^{-1} (Figure 12a). At concentrations of 0.25 and 0.5 mM, the normalized spectra of macrocycle **2** were nearly the same, which indicated that the macrocycles were present in monomeric form. Even in the monomer form (0.5 mM) some of the hydrogen-bonded N−H stretching band at 3369 cm^{-1} (red line) was present, suggesting the presence of the intramolecular hydrogen bond. This interaction was observed in crystal

(25) (a) Martin, B. R *Chem. Rev.* **1996**, *96*, 3043–3064. (b) Mido, Y.; Gohda, T. *Bull. Chem. Soc. Jpn.* **1975**, *48*, 2704–2707. (c) Jadzyn, J.; Stockhausen, M.; Zywucki, B. *J. Phys. Chem.* **1987**, *91*, 754–757. (d) Haushalter, K. A.; Lau, J.; Roberts, J. D. *J. Am. Chem. Soc.* **1996**, *118*, 8891–8896. (e) Cazacu, A.; Tong, C.; Lee, A.; Fyles, T., M.; Barboiu, M. *J. Am. Chem. Soc.* **2006**, *128*, 9541–9548.

(26) Lortie, F.; Boileau, S.; Bouteiller, L. *Chem. Eur. J.* **2003**, *9*, 3008–3014.

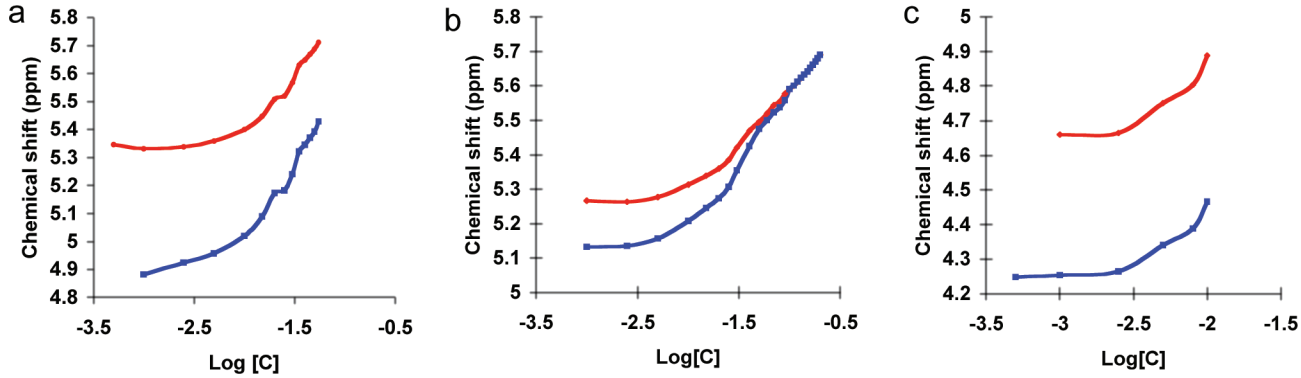

FIGURE 11. ^{1}H titration study of macrocycles (a) **2**, (b) **3**, and (c) **4** in TCE-d_2, concentration in mol/L.

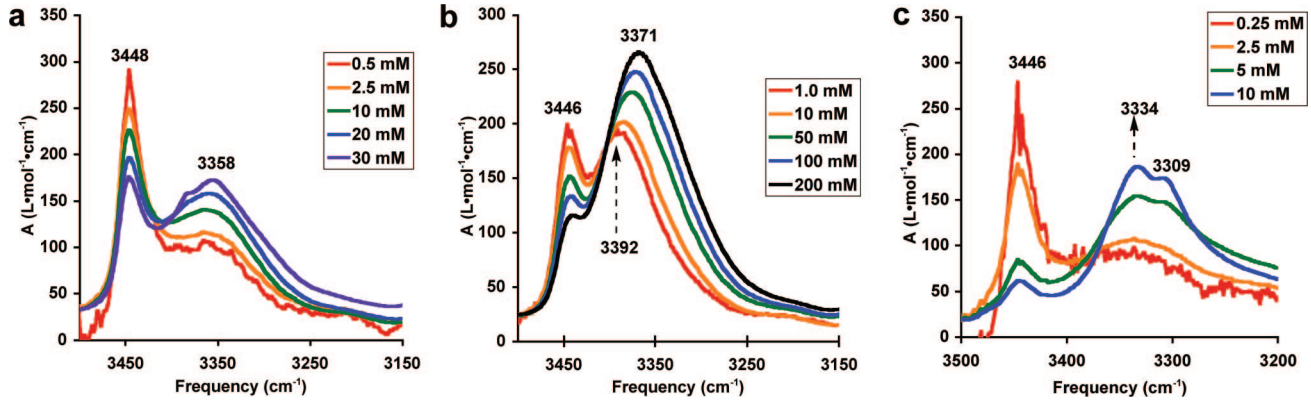

FIGURE 12. Normalized FT-IR spectra of dilution studies of (a) macrocycle **2**, (b) macrocycle **3**, and (c) macrocycle **4**.

structure of **2**. FT-IR experiments with **2** in TCE reveal a decrease in the free NH stretching band with increasing concentration. A corresponding increase in the hydrogen-bonded urea N−H band was observed with increasing concentration, which was consistent with the formation of the typical 3-centered urea hydrogen bonding interaction.

The intramolecular hydrogen bonding was more pronounced in bis-urea **3**, which had a larger hydrogen-bonded band at 3392 cm^{-1} at low concentrations (1 mM, Figure 12b). With increasing concentration, the hydrogen-bonded N−H stretch shifted from 3392 cm^{-1} to a lower frequency at 3371 cm^{-1}. This shift reflected the weakening of the intramolecular hydrogen bond in favor of the intermolecular 3-centered urea hydrogen. A marked decrease of the free N−H stretch was observed, concurrent with the intermolecular hydrogen bond formation.

Macrocycle **4** contains no ether oxygens that can act as hydrogen bond acceptors. As expected, little of the hydrogen-bonded NH stretch was observed at the lowest concentration (0.25 mM). FT-IR studies of macrocycle displayed two free urea N−H stretching two frequencies at 3446 and 3443 cm^{-1}, which corresponded to the *m*-xylene NH and the octyl NH. Again, the free NH bands decreased with increasing concentration (Figure 12c). An increase in the two frequencies at 3334 and 3309 cm^{-1} for hydrogen-bonded urea N−H stretching was observed with increasing concentration.

We used these FT-IR studies to estimate the association constants for macrocycles **2**−**4** using eqs 1−3. The first association to form a dimer (K_2, eq 1) was treated separately from the oligomerization constant. We believed that dimerization should be unfavorable due to entropic costs. The addition of successive molecules was described using a common association constant (K, eq 2).[24,25] Jadzyn and Bouteiller utilized this method

TABLE 2. Comparison of Association Constants for Bis-urea Macrocycles (2−4) versus Bis-urea Supramolecular Polymers (7−8)[27]

compound	K_2 (M^{-1})	K (M^{-1})	solvent
2	39	36	TCE
3	13	5	TCE
4	30	600	TCE
7	7	2300	$CHCl_3$
8	21	1400	$CHCl_3$

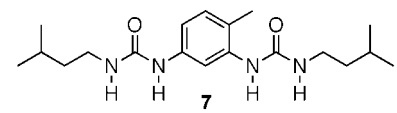

7

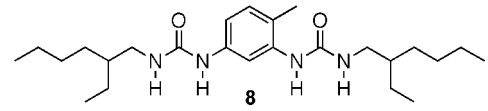

8

to calculate the dimerization constant K_2 and association constant K of acyclic bis-ureas **7** and **8** (Table 2). Bouteiller estimated dimerization constants in chloroform of $K_2 = 7-21$ M^{-1}, which reflect the entropic costs of forming the dimer.[27] Our dimerization constants are in the same range ($K_2 = 13-39$ M^{-1}).

$$A_1 + A_1 \overset{K_2}{\rightleftharpoons} A_2 \quad (1)$$

$$A_1 + A_1 \overset{K_2}{\rightleftharpoons} A_{i+1}; i = 2, 3, 4, \text{ etc.} \quad (2)$$

(27) Simic, V.; Bouteiller, L.; Jalabert, M. *J. Am. Chem. Soc.* **2003**, *125*, 13148–13154.

$$K_2 = \left(\frac{C_2}{C_1^2}\right) \neq K_3 = K_4 = \ldots = K_i = k = \left(\frac{C_{i+1}}{C_1 C_i}\right) \quad (3)$$

Table 2 lists the calculated association constants for macrocycles **2**−**4** in TCE compared with **7** and **8** in $CHCl_3$, two bis-ureas that are reported to assemble into supramolecular polymers.[27] In comparison our macrocyclic bis-ureas showed much lower association constants for the oligomerization ($K = 5-600$ M^{-1}) than versus the acyclic bis-ureas, which displayed K values of ~1900 M^{-1}. The lower association constants of the ethylene glycol containing macrocycles **2** ($K = 36$ M^{-1}) and **3** ($K = 5$ M^{-1}) may reflect the strength of the intramolecular hydrogen bond to the ether oxygens in **2** and **3**, which must be broken before the dimers can further associate. We expect hydrogen bonding to be stronger in chloroform than TCE; however, our macrocycles were not soluble enough in chloroform to probe their IR over a reasonable concentration range. Although these solution studies do not address the actual structures of the dimer or oligomeric assemblies they do suggest that these monomers associate through the typical 3-centered urea hydrogen-bonding motif.

Conclusions

In conclusion, we found that we were able to synthesize the unsymmetrical bis-urea macrocycles in higher yields without the need of protecting groups on the urea moieties. These unsymmetrical systems were indeed more soluble in most organic solvents. Solution studies indicated that the higher solubility came primarily from a decrease in their association constants. In the case of the ether containing macrocycles, the monomers also showed clear IR stretches that were associated with hydrogen-bonded N−H stretching band, suggesting the presence of an intramolecular hydrogen bond within the macrocycle. Presumably this intramolecular hydrogen bond must be broken or weakened for intermolecular association to begin.

Solid-state studies showed us that for the unsymmetrical bis-urea macrocycles offset structures were more prevalent than columnar assembly. The flexibility of these systems and the inclusion of the ether oxygens gave rise to many additional assembly patterns. Energetically, these patterns must be quite similar as subtle changes such as the inclusion of a single methyl group shifted the structure from one assembly pattern to another. Although the flexible macrocycles can form a wider range of structures, we were still able to observe the desired columns. Our studies suggest that the rigid arene spacers of our initial symmetrical bis-ureas were quite important in forming columnar assembly. They also suggest that heteroatoms may be included within a rigid framework. Given these observations, we are currently exploring the use of heterocyclic aryl spacers, which rigidly position the heteroatoms within the macrocyclic framework. Columnar assembly of such building blocks could give porous materials with channels that are lined with functionality for molecular recognition and potentially for catalysis.

Experimental Section

General Procedure for the Synthesis of Bis-ureas 2−6. Synthesis of Macrocycle 2. An oven-dried three-neck round-bottom flask was filled with 400 mL of anhydrous DMF, and the mixture was stirred under N_2 atmosphere and cooled in ice bath. Two separate addition funnels were charged with solutions of 2,2′-(ethylenedioxy)diethylamine (0.22 mL, 1.5 mmol) in 50 mL of DMF and *m*-xylylene diisocyanates (0.235 mL, 1.5 mmol) in 50 mL of DMF. The diamines and diisocyanate solutions were added together dropwise over ~30 min and further stirred at room temperature for 72 h. The reaction was reduced in vacuo, and the product was purified by column chromatography on silica (10:1 CH_2Cl_2/methanol) to give macrocycle **2** (0.36 g, 72% yield): white solid; mp 247−250 °C; ^{1}H (DMSO-d_6) δ 3.16, (m, 4H), 3.45, (t, J = 6.2 Hz, 4H), 3.53, (s, 4H), 4.22, (d, J = 6.0 Hz, 4H), 5.93, (t, J = 5.4 Hz, 2H), 6.42, (t, J = 6.0 Hz, 2H), 7.02, (d, J = 7.2 Hz, 2H), 7.16, (t, J = 7.4 Hz, 1H), 7.20, (s, 1H); ^{13}C NMR δ 40.3, 43.2, 70.65, 70.71, 124.1, 126.0, 128.3, 141.9, 158.6; MS *m*/*z* (ES) 337 (MH^+, 100); HRMS calcd for $C_{16}H_{25}N_4O_4$ (MH^+) 337.1876, found 337.1877. The other macrocycles were synthesized by a similar method (see Supporting Information).

Acknowledgment. The authors gratefully acknowledge support in part for this work from the NSF (CHE-071817), from the Petroleum Research Fund (44682), and from a grant from the University of South Carolina, Office of Research and Health Sciences.

Supporting Information Available: ^{1}H and ^{13}C NMR spectra of all new compounds; X-ray crystallographic files in CIF format for **2**, **4**, **5**, and **6**; ^{1}H and FT-IR titration of **2**, **3**, and **4**. This material is available free of charge via the Internet at http://pubs.acs.org.

JO801717W